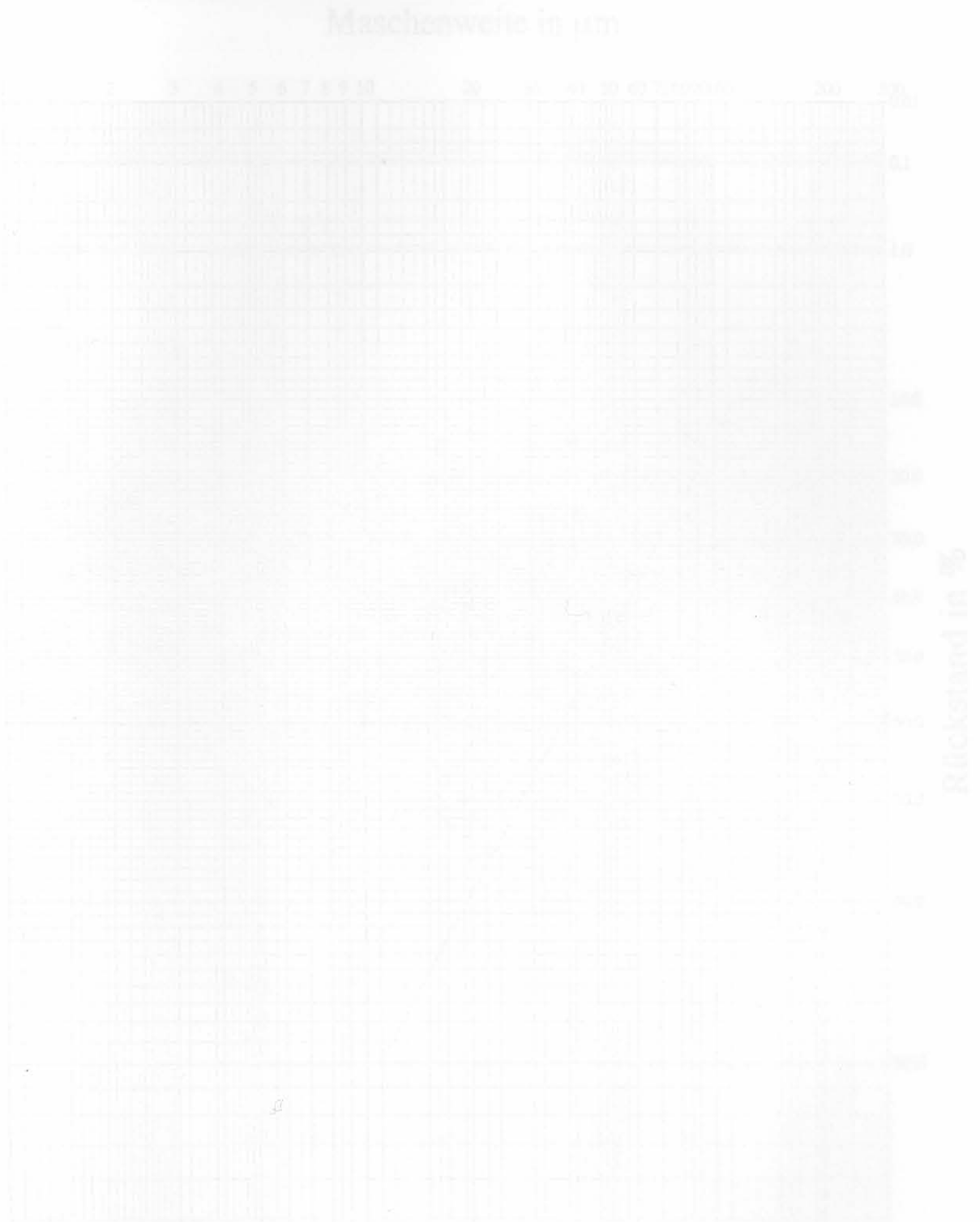


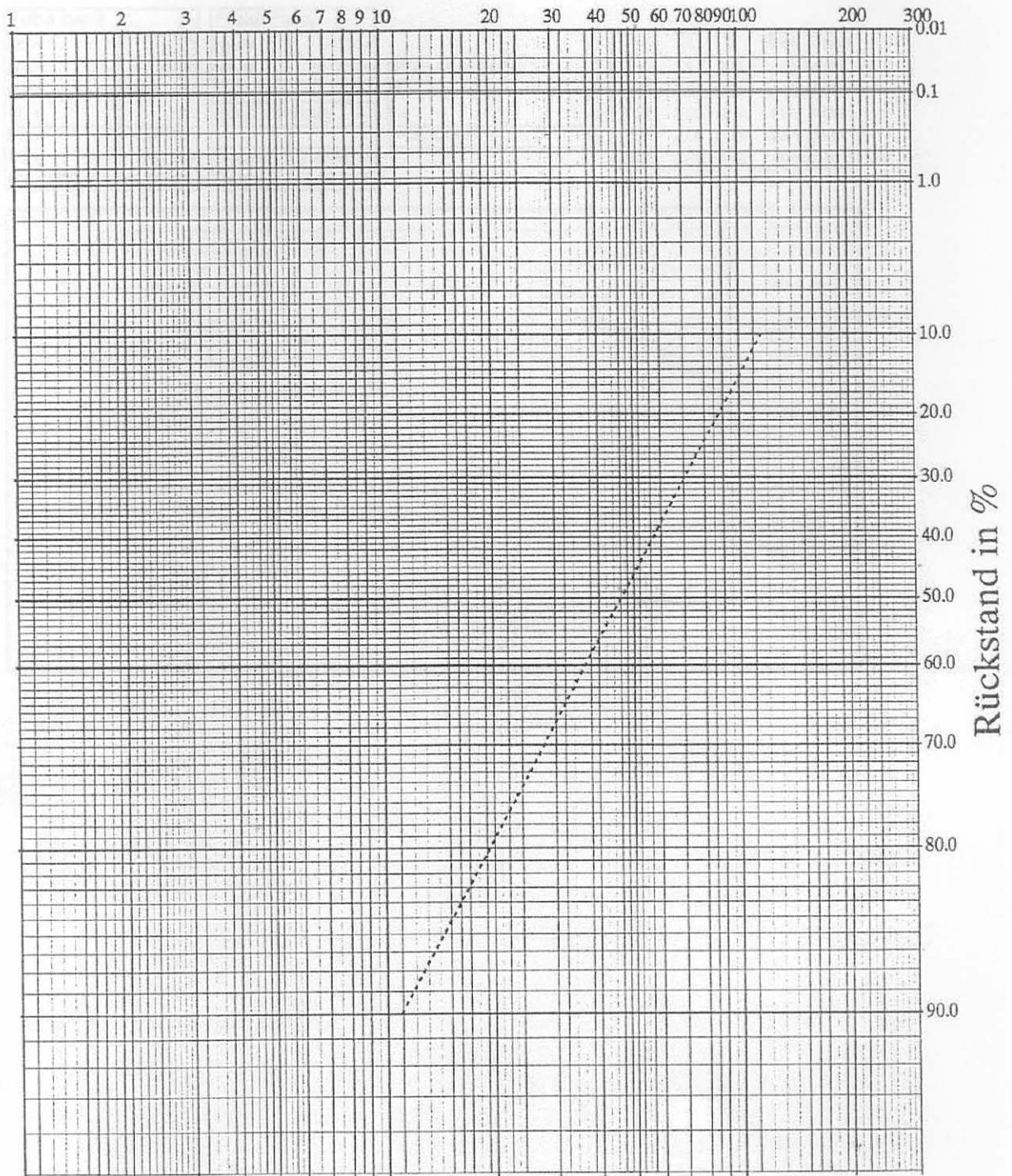
Appendices

Fly-Ash Particle Sizes



Appendix A - Fly-Ash Particle Sizes

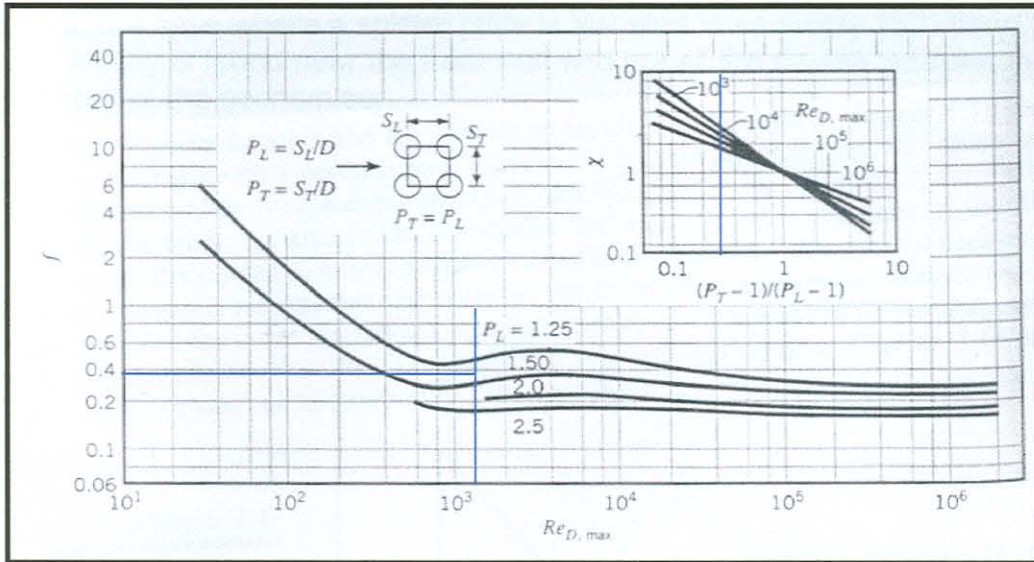
Maschenweite in μm



Appendix B - Tube Bank Pressure Drop Calculation

Tube Bank Pressure Drop Calculation - Zukauskas

| Tube bank | | Fluid Prop. | | Pressure Drop | | V X f Pres Drop | | | |
|----------------|----------|----------------|-----------|---------------|------------|-----------------|------|------|-----------|
| NL = | 13 | rho = | 0.354 | X = | 3 | 1 | 3 | 0.4 | 16.6417 |
| D = | 88.9 | mu = | 4.15E-05 | f = | 0.4 | 4 | 2.05 | 0.35 | 159.2057 |
| ST = | 150 | Inlet Velocity | | Pres. Drop = | 16.6417105 | 10 | 2.05 | 0.4 | 1137.1836 |
| SL = | 120 | v = | 1 | | | 17 | 2.05 | 0.35 | 2875.6529 |
| PL = | 1.349831 | vmax = | 2.4549918 | | | 25 | 2.05 | 0.32 | 5685.918 |
| PT = | 1.687289 | Re = | 1.86E+03 | | | | | | |
| (PL-1)(PT-1) = | 0.240435 | | | | | | | | |



Appendix C - Concepts to Alleviate Airheater Erosion

This appendix discusses different flow-modification remedial measure concepts for airheater tube erosion. The two most successful approaches were discussed in Chapter 5.4.

Concept 1: Splitter Plate

As discussed in Chapter 3.5, Tu et al. [48] proposed the installation of a splitter plate in boilers with an empty 180° bend by providing a longer flow path at the bend. In the case where a splitter plate is installed in an empty 180° bend, the peak velocity is found near the front wall and not all the fly-ash particles move to the rear of the economiser.

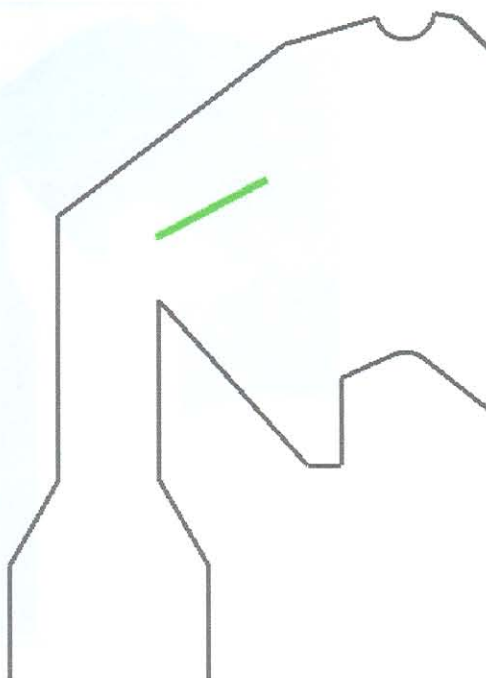


Figure C-1 Concept 1: Location of Splitter Plate

The location of the splitter plate used in this study is illustrated in Figure C-1. Through the use of this flow-modifying device it is hoped to obtain a uniform particle distribution in the airheater with low peak velocities. Figure C-2 illustrates the velocity magnitude contour plot for the case where the splitter plate is included in the CFD model. It can be seen from Figure C-2 that the maximum velocity in the flow domain for the chosen inlet boundary conditions is $13.22\text{m}\cdot\text{s}^{-1}$. If this velocity is compared to Figure 5-27, the case without any flow-modifying devices, it can be seen that the maximum velocity increased by almost 10% from $12.03\text{m}\cdot\text{s}^{-1}$. The location of the maximum velocity is in the same position for both cases. Therefore, the splitter plate is ineffective in reducing the maximum velocity.

The other parameter of erosion that can be altered by flow-modifying approaches is the particle concentration. Figure C-3 and Figure C-4 illustrate the particle trajectories for 100 μm and 10 μm particles respectively. If this results are compared to Figure 4-15 and Figure 4-14, the case where no flow-modifying were used, it can be seen that there are no major differences in the particle trajectories for the different cases.

It can thus be concluded that the splitter plate is ineffective in redistributing the flow in such a manner that the particle concentration is uniform across the airheater. The maximum velocity in the flow domain also increased as a result of the splitter plate. As splitter plate parameters such as the size, shape and location of the splitter plate was arbitrarily chosen, other parameters can result in better results. Mathematical optimisation can be used in achieving this.

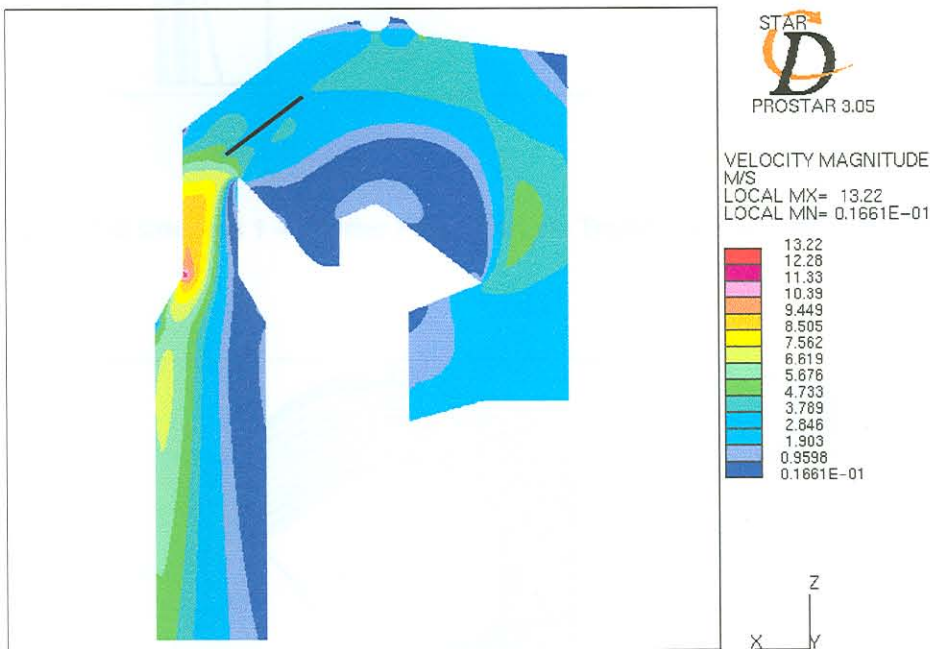


Figure C-2 Concept 1 – Splitter Plate: Velocity Magnitude Plot ($2\text{m}\cdot\text{s}^{-1}$ Inlet Velocity)

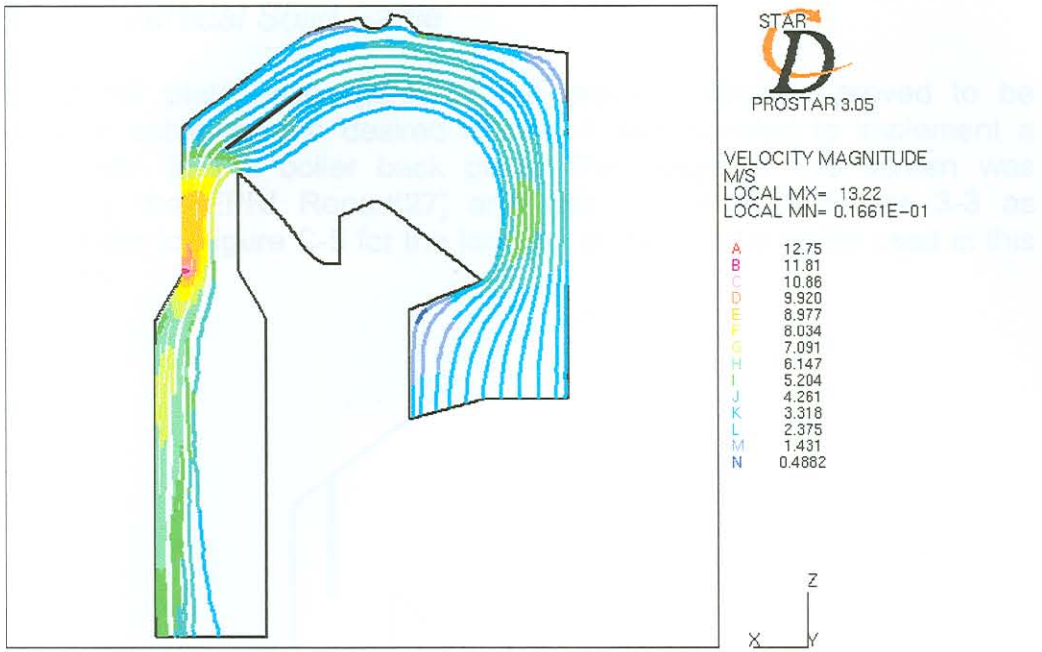


Figure C-3 Concept 1 – Splitter Plate: Particle Trajectories of 100µm Particles



Figure C-4 Concept 1 – Splitter Plate: Particle Trajectories of 10µm Particles

Concept 2: Vertical Solid Baffle

As the splitter plate, investigated in the previous section, proved to be ineffective in achieving the desired results, it was decided to implement a vertical screen in the boiler back pass. The usage of this screen was proposed by the EPRI Report[27] and was illustrated in Figure 3-3 as Screen I. Refer to Figure C-5 for the location of the vertical baffle used in this investigation.

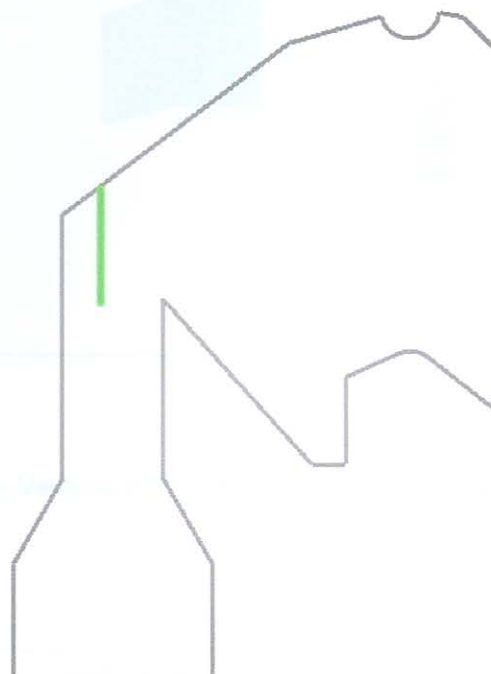


Figure C-5 Concept 2: Location of Vertical Baffle

The velocity magnitude contour plot is illustrated in Figure C-6 for this case. The maximum velocity in the flow domain for the chosen inlet boundary conditions is $13.98\text{m}\cdot\text{s}^{-1}$. This is a 16% increase in the maximum velocity from when no flow-modifying devices are used. The location of the high peak velocity is not near the back wall anymore. However, it is now located at the lower top of the vertical baffle. Boiler wall and baffle erosion can therefore occur in that region.

Particle trajectories for $100\mu\text{m}$ and $10\mu\text{m}$ particles can be seen in Figure C-7 and Figure C-8 respectively. The results obtained from this analysis are even worse than those obtained when no flow-modifying devices were used. The particle concentration is high only on the one side of the airheater, with a possible concentration of tube failures there.

In conclusion, the vertical solid baffle is not suited as a remedial measure for airheater tube erosion. This baffle will rather exacerbate tube erosion in the airheater.

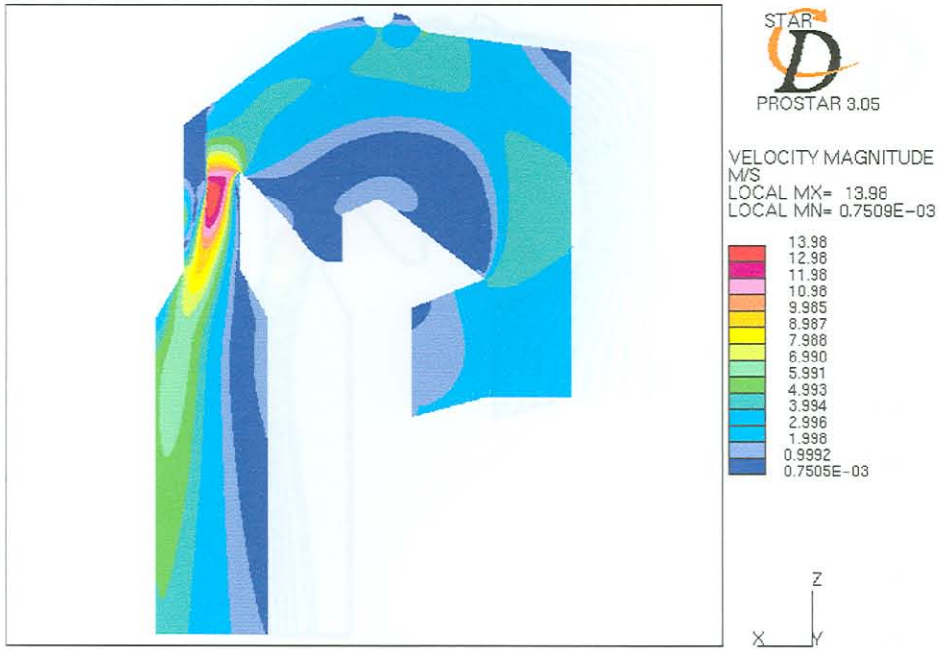


Figure C-6 Concept 2 – Vertical Solid Baffle: Velocity Magnitude Contour Plot (2m.s⁻¹ Inlet Velocity)



Figure C-7 Concept 2 – Vertical Solid Baffle: Particle Trajectories of 100µm Particles



Figure C-8 Concept 2 – Vertical Solid Baffle: Particle Trajectories of 10 μ m Particles

Concept 3: Permeable Baffle to Cover Entire Flow Area

The third concept proposed entails the usage of a permeable baffle across the entire inlet passage of the airheater. This baffle will hopefully redistribute the flow and fly-ash particles uniformly across the airheater. The location of the permeable baffle is illustrated in Figure C-9.

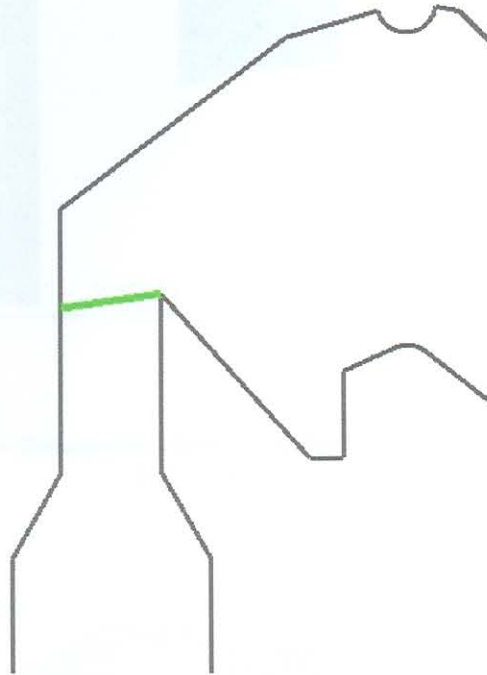


Figure C-9 Concept 3: Location of Baffle to Cover Entire Flow Area

It can be seen from Figure C-10 that the baffle has no major effect on the flow pattern through the airheater. There still exists a large recirculation zone in one side of the airheater. The maximum velocity in the flow is $10.09\text{m}\cdot\text{s}^{-1}$, which is a 16% drop from the case where no flow-modifying devices were used. This is encouraging but with an expense of pressure drop across the baffle.

From Figure C-11 and Figure C-12, which illustrate the particle trajectories for $100\mu\text{m}$ and $10\mu\text{m}$ respectively, it can be seen that the baffle is still ineffective to provide a uniform particle distribution across the airheater.

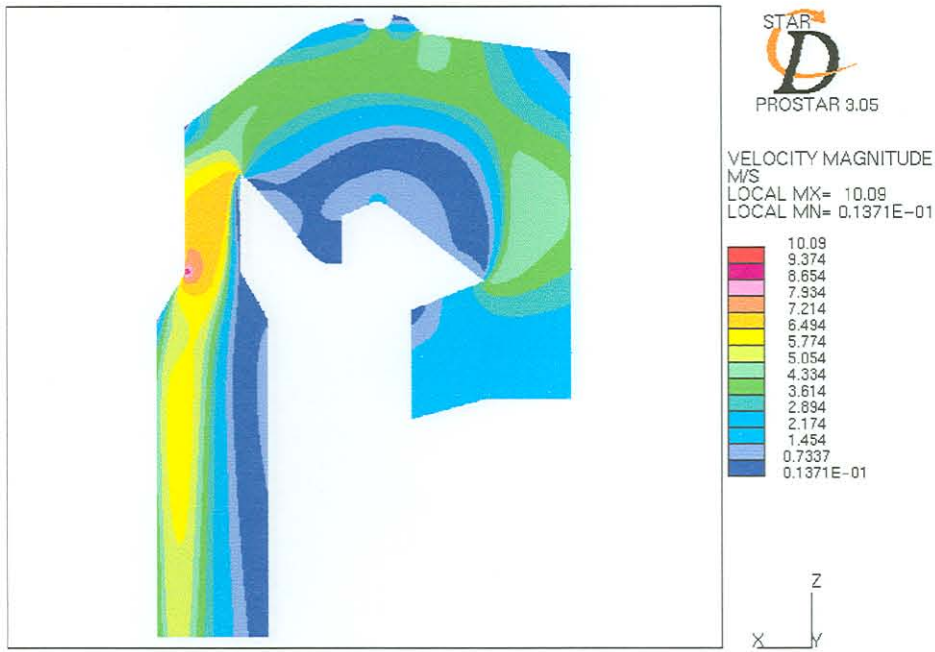


Figure C-10 Concept 3 – Permeable Horizontal Baffle: Velocity Magnitude Contour Plot (2m.s⁻¹ Inlet Velocity)



Figure C-11 Concept 3 – Permeable Horizontal Baffle: Particle Trajectories of 100µm Particles

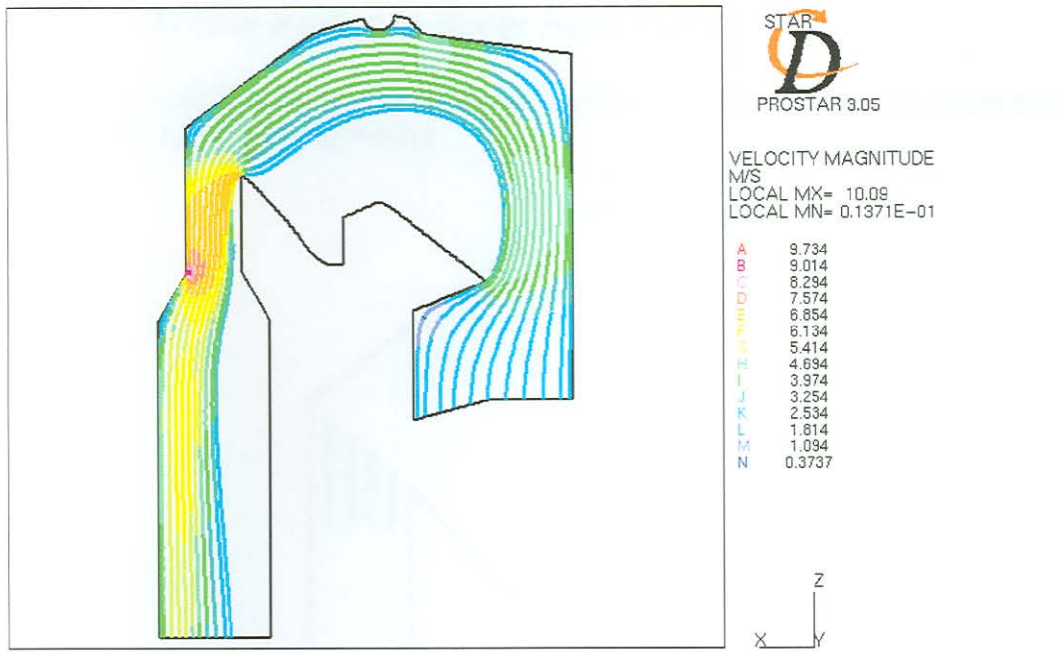


Figure C-12 Concept 3 – Permeable Horizontal Baffle: Particle Trajectories of 10µm Particles

Concept 4: Multiple Baffles in Boiler Back Pass

Figure C-13 illustrates the location of four baffles of different sizes to direct the flow uniformly across the airheater.



Figure C-13 Concept 4: Location of Multiple Baffles in Boiler Back Pass

Figure C-14 illustrates the velocity magnitude contour plot for this flow-modifying concept. The maximum velocity in the flow domain is $9.27\text{m}\cdot\text{s}^{-1}$ for the given inlet boundary conditions. This translates into a 23% decrease in the maximum velocity for the case without flow-modifying devices and a 14% increase from the concept of the permeable baffle investigated in the previous section. However, the region of high peak velocity is at the top of the boiler between the baffle plates and is far from the airheater tubes.

The particle trajectories are shown in Figure C-15 and Figure C-16 for $100\mu\text{m}$ and $10\mu\text{m}$ particles respectively. The uniformity of the particles across the airheater is not as uniform as the particles from the previous section but is better than all the other concepts investigated thus far in this appendix.



Figure C-14 Concept 4 – Vertical Baffles: Velocity Magnitude Contour Plot ($2\text{m}\cdot\text{s}^{-1}$ Inlet Velocity)

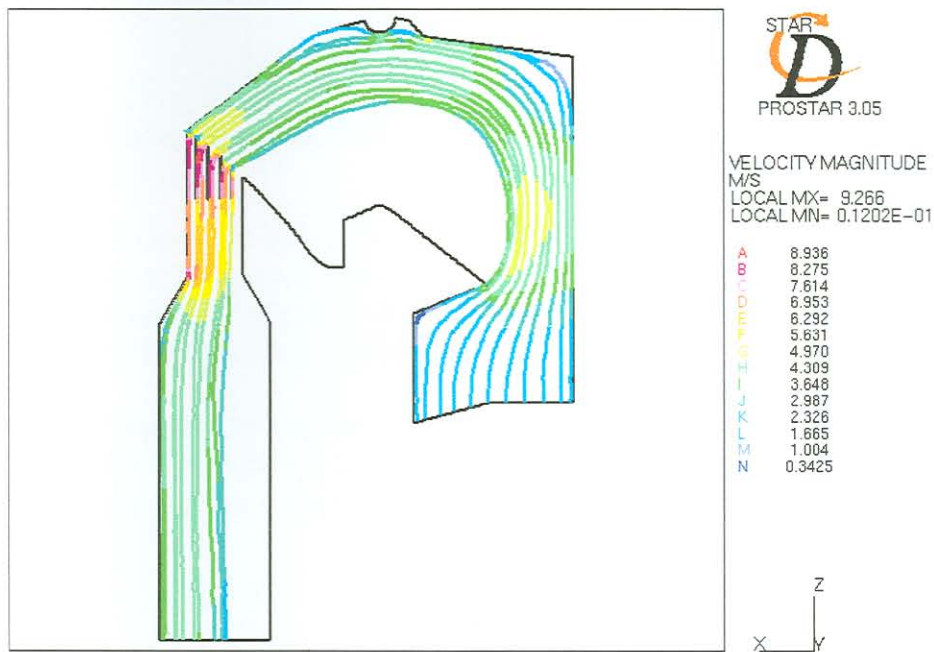


Figure C-15 Concept 4 – Vertical Baffles: Particle Trajectories of $100\mu\text{m}$ Particles

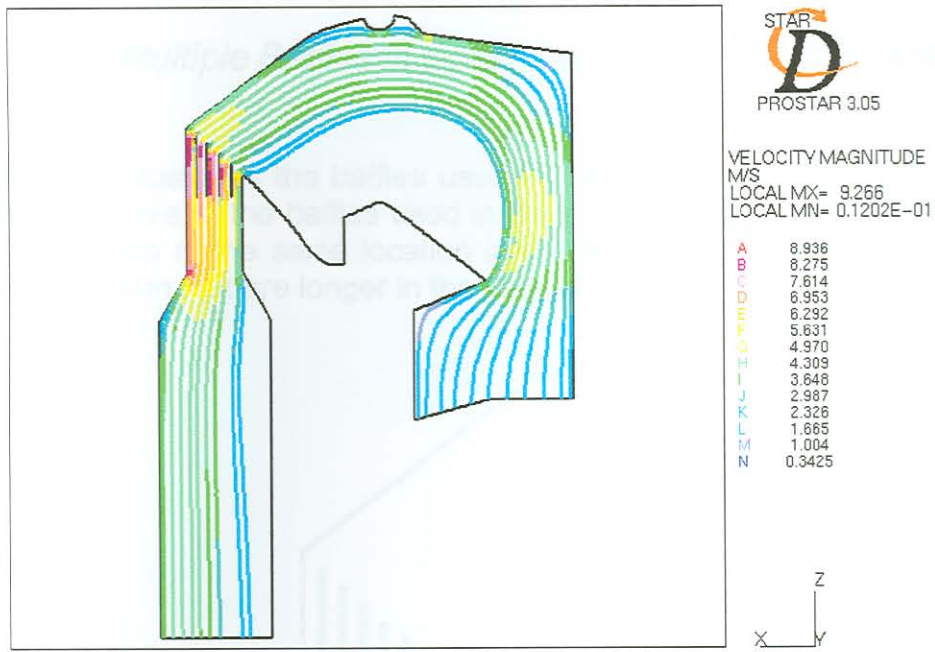


Figure C-16 Concept 4 – Vertical Baffles: Particle Trajectories of $10\mu\text{m}$ Particles

Concept 5: Multiple Baffles in Boiler Back Pass – Modification to Concept 4

Figure C-17 illustrates the baffles used in the CFD model to investigate the effect of the size of the baffles used in the previous section on the flow field. The baffles are at the same location in the boiler than the ones used in the previous section, but are longer in the vertical direction.

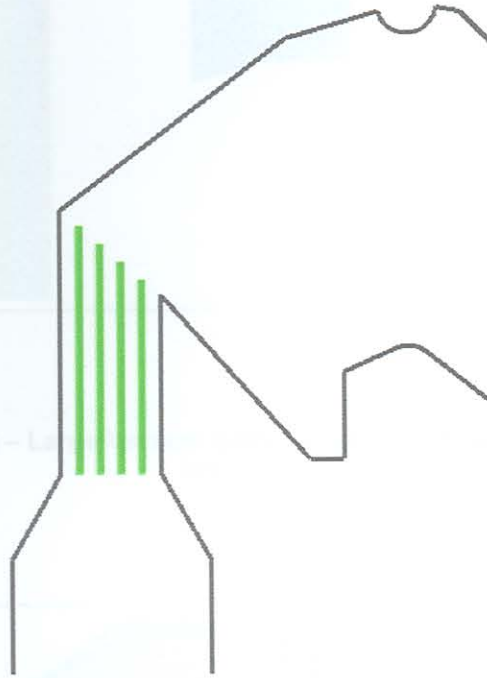


Figure C-17 Concept 5: Multiple Baffles in Boiler Back Pass – Modification to Concept 6

Figure C-18 illustrates the velocity magnitude contour plot for the CFD model with the baffles illustrated in Figure C-17. The maximum velocity in the flow domain increased by 5% from the maximum velocity in the previous concept, where smaller baffles were used.

The effect of the larger baffles on particle trajectories is minor as compared to the case with the smaller baffles. The particle trajectories for 100 μm and 10 μm particles can be seen in Figure C-19 and Figure C-20 respectively.



Figure C-18 Concept 5 – Large Vertical Baffles: Velocity Magnitude Contour Plot (2m.s⁻¹ Inlet Velocity)

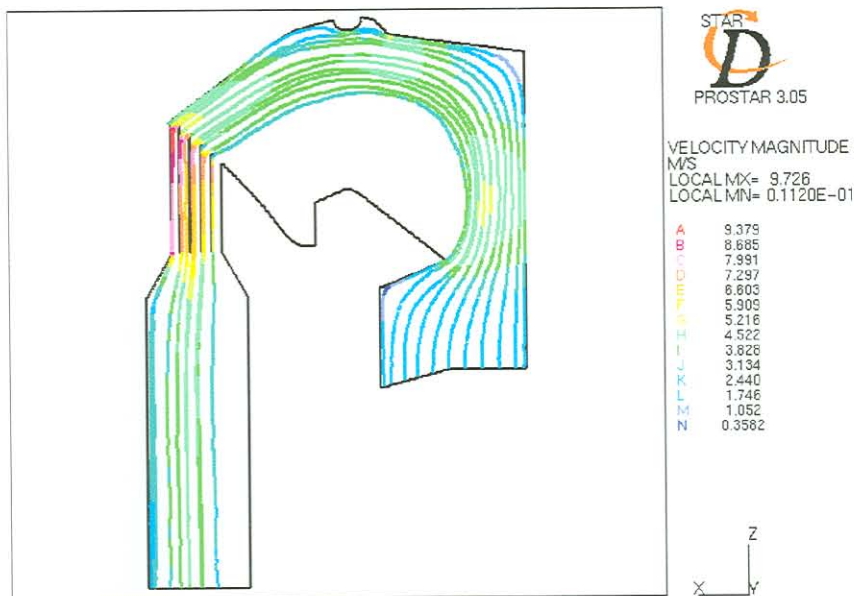


Figure C-19 Concept 5 – Large Vertical Baffles: Particle Trajectories of 100µm Particles

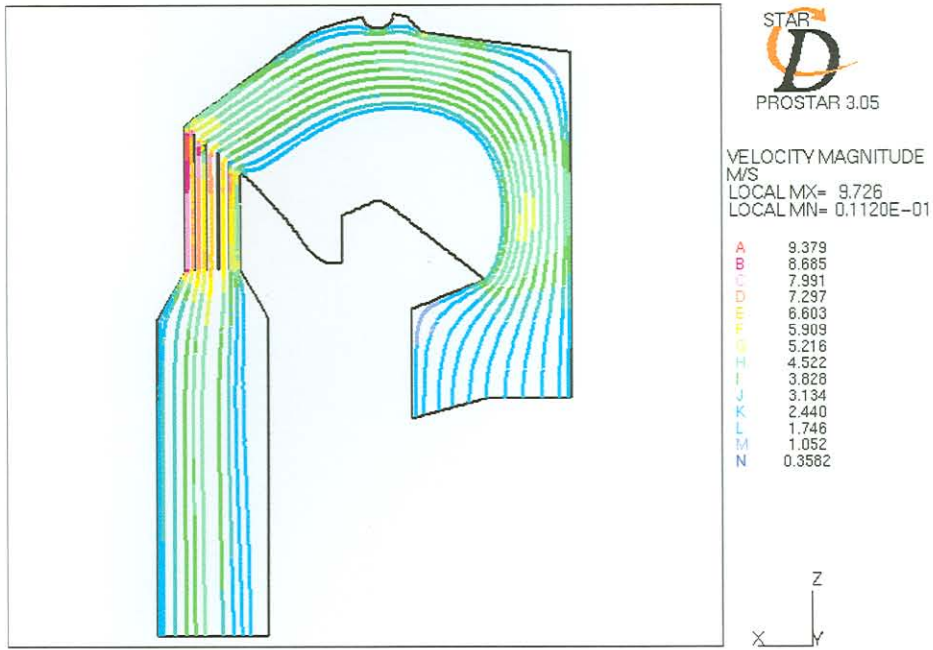


Figure C-20 Concept 5- Large Vertical Baffles: Particle Trajectories of 10µm Particles